PHYSICAL REVIEW A **84**, 051802(R) (2011)

High-brightness switchable multiwavelength remote laser in air

Jinping Yao,[1] Bin Zeng,[1,3] Huailiang Xu,[2,*] Guihua Li,[1,3] Wei Chu,[1,3] Jielei Ni,[1,3] Haisu Zhang,[1,3] See Leang Chin,[4] Ya Cheng,[1,†] and Zhizhan Xu[1,‡]

[1]*State Key Laboratory of High Field Laser Physics, Shanghai Institute of Optics and Fine Mechanics, Chinese Academy of Sciences, Shanghai 201800, China*

[2]*State Key Laboratory on Integrated Optoelectronics, College of Electronic Science and Engineering, Jilin University, Changchun 130012, China*

[3]*Graduate School of Chinese Academy of Sciences, Beijing 100080, China*

[4]*Center for Optics, Université Laval, Quebec City, Quebec G1V 0A6, Canada*

(Received 29 May 2011; published 15 November 2011)

We demonstrate a harmonic-seeded switchable multiwavelength laser in air driven by intense midinfrared femtosecond laser pulses, in which population inversion occurs at an ultrafast time scale (i.e., less than ∼200 fs) owing to direct formation of excited molecular nitrogen ions by strong-field ionization of inner-valence electrons. The bright multiwavelength laser in air opens the perspective for remote detection of multiple pollutants based on nonlinear optical spectroscopy.

DOI: 10.1103/PhysRevA.84.051802 PACS number(s): 42.65.Re

A remote laser in air based on amplified spontaneous emission (ASE) has produced rather well-collimated coherent beams in both backward and forward propagation directions [1–3], opening up possibilities for remote sensing approaches [4,5]. Remote ASE-based lasers were shown to enable operation at both ∼391 and 337 nm using molecular nitrogen or at ∼845 nm using molecular oxygen as the gain medium, depending on the employed pump lasers. To date, and to the best of our knowledge, a multiwavelength laser in air that allows for dynamically switching the operating wavelength has not yet been achieved, although this type of laser is certainly of high importance for detecting multiple hazard gases [6].

Femtosecond laser filamentation [7–9] not only gives rise to an extended spatial confinement of the femtosecond laser beam, but also a high peak intensity stabilized inside the filament core due to the well-known intensity clamping effect [10–12]. Both these effects can be beneficial for enhancing the efficiency of nonlinear optical processes, such as third harmonic generation and four-wave mixing [13–15]. In particular, ASEs of nitrogen molecules at 337 and 391 nm and that of oxygen atoms at 845 nm have been observed in the femtosecond-laser-induced plasma filament in air. Although the nitrogen-based remote laser can potentially operate at multiple wavelengths as conventional nitrogen lasers do, switching between different wavelengths by use of optics is difficult owing to the fact that the remote lasing action always occurs far from the pump laser system. We show that this problem can be circumvented by seeding the nitrogen laser in air with self-generated harmonics of an ultrafast wavelength-tunable midinfrared (mid-IR) pump laser. The consequence is a tunable highly amplified seed laser but not an ASE-based laser.

The remote lasing action was demonstrated with wavelength-tunable mid-IR laser pulses generated from an optical parametric amplifier (OPA, HE-TOPAS, Light Conversion, Inc.), which was pumped by a commercial Ti:sapphire laser system (Legend Elite-Duo, Coherent, Inc.). These intense mid-IR laser pulses have enabled investigation of strong field atomic physics, such as above threshold ionization and high-order harmonic generation [16,17]. The central wavelength of the mid-IR pulses can be continuously tuned in the spectral range from ∼1200 to 2500 nm. In the spectral range of 1600–2500 nm, which corresponds to the idler output of OPA, the maximum pulse energy of the OPA could reach ∼700 μJ, and a pulse duration of ∼1900 nm was measured to be ∼200 fs. The pump laser pulses were focused into air using lenses of different focal lengths ranging from 36 to 300 mm to generate the third and fifth harmonics as well as the remote laser in air. A grating spectrometer (Shamrock 303i, Andor) with a 1200 grooves/mm grating was used to record the spectra of both neutral and ionized nitrogen molecules. To measure the fluorescence spectra in the backward or side directions, a fiber head was used to collect the signal into the grating spectrometer. In this case, a focal lens was used to couple the fluorescence light into the fiber head.

Figure 1(a) shows the remote laser spectrum obtained by focusing ∼500-μJ, ∼200-fs, 1900-nm pump pulses in air with a lens of 36-mm focal length (e.g., the peak intensity at the geometrical focus is $\sim 5.6 \times 10^{14}$ W/cm^2, if we assume the pulses are focused into vacuum). Although the unknown clamped intensity in the filament would be lower, it would not be too low and would be of the order of $\sim 10^{14}$ W/cm^2. Unlike the typical supercontinuum-like spectra of the third and fifth harmonics that are produced by filamentation of mid-IR laser pulses [12], a strong, narrow-bandwidth emission at 391 nm appears on top of the spectrum of the fifth harmonic, whose intensity is nearly two to three orders of magnitude higher than that of the fluorescence lines at 357 and 337 nm from neutral molecular nitrogen. In addition, we examined the polarization of the emission at 391 nm using a Glan-Taylor polarizer, which was placed just before the spectrometer. As shown in the inset of Fig. 1(a), the strong emission at 391 nm is nearly perfectly linearly polarized in the direction parallel to that of the pump pulse. This provides strong

*huailiang@jlu.edu.cn
†ya.cheng@siom.ac.cn
‡zzxu@mail.shcnc.ac.cn

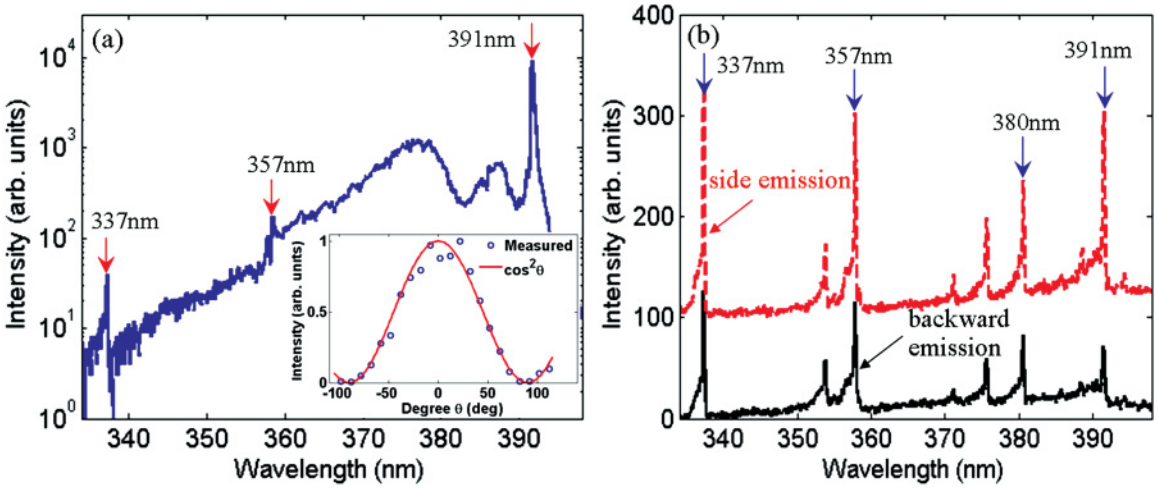

FIG. 1. (Color online) Typical spectra of nitrogen excited by 1900-nm laser pulses recorded in (a) forward, (b) backward (black solid line), and side (red dashed line) directions. Inset in (a): Polarization property of remote laser at ∼391 nm. Dashed curves are vertically shifted in (b) for clarity.

evidence on the harmonic seed being amplified (lasing action) at 391 nm because both spontaneous emission and ASE will show isotropic polarization. For comparison, we also present the fluorescence spectra measured for the backward and side emissions, as shown by the solid and dashed curves in Fig. 1(b). Since the seeding effect cannot take place in these directions as the fifth harmonic beam always follows the laser propagation in the forward direction, the spectra recorded in the backward and side directions do not show any lasing peak as the 391 nm laser in Fig. 1(a); they appear similar to each other, as shown in Fig. 1(b), in which only fluorescence lines of comparable intensities from both ionized and neutral nitrogen molecules are observed.

The seeding effect due to the existence of the fifth harmonic in the gain zone is further confirmed by examining the spectra of the remote laser at 391 nm for different pump wavelengths, as shown in Fig. 2(a). When the pump wavelength is tuned to 1906 nm, the intensity of the 391-nm laser is the strongest; however, when the pump wavelength is tuned toward either the longer or the shorter wavelength, the intensity of the 391-nm laser decreases significantly, as shown in Fig. 2(a). Furthermore, as shown in Fig. 2(b), harmonic-seeded remote lasers can also be realized at multiple wavelengths of 330, 357, 391, 428, and 471 nm, which correspond to the transitions between different vibrational levels of the electronic $B\,^2\Sigma_u^+$ and $X\,^2\Sigma_g^+$ states of molecular nitrogen ions (see Fig. 5 below), when the pump wavelengths are, respectively, tuned to 1682, 1760, 1920, 2050, and 1415 nm. It should be noted that since the pump pulse energy of our mid-IR OPA source drops significantly for a wavelength of longer than 2200 nm, the remote lasing action at 471 nm is thus seeded by the third harmonic of the pump pulses.

As a final evidence on the population inversion, we show that the seeded lasing action at 391 nm can also be achieved with externally injected seed pulses offered by the second harmonic of the 800-nm Ti:sapphire laser. In particular, the second harmonic is polarized in the direction perpendicular to that of the mid-IR pump pulses, so that it can be easily separated from the self-generated fifth harmonic using a Glan-Taylor polarizer. The ∼0.3-μJ, ∼40-fs second harmonic was combined with the 1920-nm pump pulses by use of a dichroic mirror with high reflectivity at 400 nm and high transmission at 1920 nm, and then the collinearly propagating pump pulses at 1920 nm and seed pulses at 400 nm were both focused into air by a 36-mm focal-length plano-convex lens to produce the plasma channel. The temporal synchronization between the second harmonic and the pump pulses was

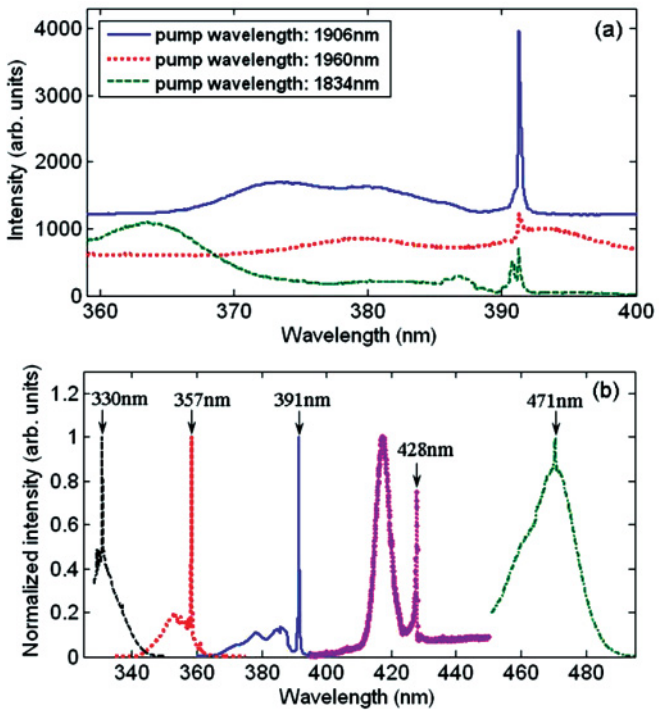

FIG. 2. (Color online) (a) Measured spectra of remote laser at 391 nm for different pump wavelengths of 1834, 1906, and 1960 nm, and (b) the lasing peaks at 471, 428, 391, 357, and 330 nm achieved with different pump wavelengths of 1415, 2050, 1920, 1760, and 1682 nm, respectively. Curves are shifted vertically in (a) for clarity.

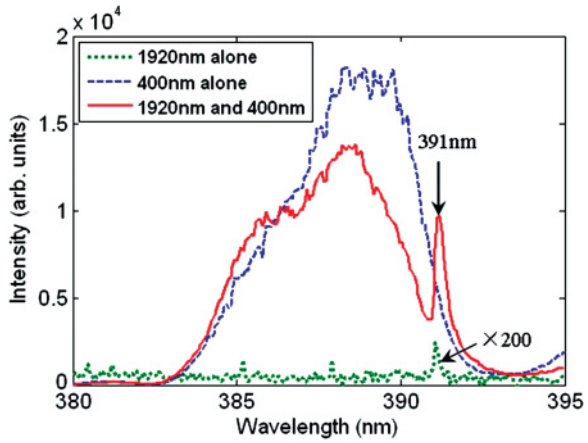

FIG. 3. (Color online) Spectra of externally injected second harmonic of an 800-nm Ti:sapphire laser measured before (blue dashed) and after (red solid) switching on the 1920-nm pump laser, and the spectrum obtained with only 1920-nm pump pulses (green dotted).

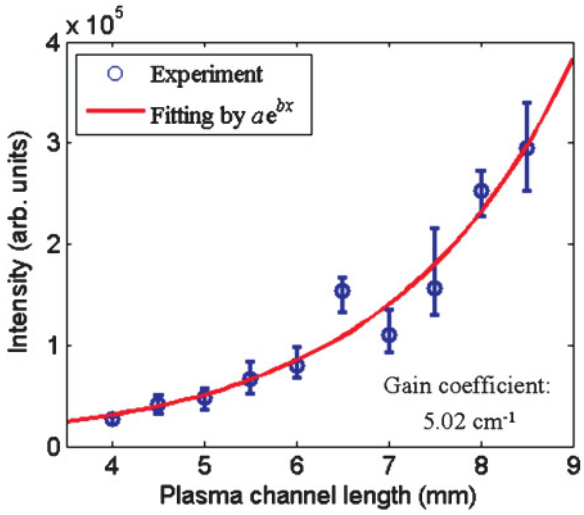

FIG. 4. (Color online) Fitted gain curve of harmonic-seeded remote laser in air at ∼391 nm.

achieved using a time-delay line. Since the lasing signal is sensitive to the wavelength of external seed, we rotated the beta barium borate (BBO) crystal and slightly shifted the central wavelength of the second harmonic to lower than 400 nm to obtain the strongest lasing signal. Figure 3 shows the spectra of the second harmonic measured before (blue dashed curve) and after (red solid curve) switching on the mid-IR pump laser. Similar to the remote laser seeded with the fifth harmonic, the 391-nm peak appears on the second harmonic spectrum when the pump laser is switched on and the spatiotemporal overlap between the second harmonic and the pump laser have been achieved. In addition, when the second harmonic is blocked while the mid-IR pump laser is still on, only a typical fluorescence spectrum of ionized and neutral nitrogen molecules is recorded, as shown by the green dotted curve in Fig. 3. Thus, injection of seed pulses is necessary to achieve lasing action.

The gain curve of the remote laser at the wavelength of 391 nm can be obtained by truncating the plasma channel using a pair of uncoated fused silica plates [13] and measuring the energy of the 391-nm laser at each truncation location. Details of the beam truncation optics can be found elsewhere [18]. Both signals of the 391-nm laser and fifth harmonic were recorded using the spectrometer (Shamrock 303i, Andor), and the energy of 391-nm laser was estimated by integrating the spectral flux over a narrow window from 391 to 392 nm. The recorded laser spectrum is peaked at 391.4 nm with a spectral width of ∼0.3 nm [full width at half maximum (FWHM)]. To remove the fluorescence signal, a polarizer was placed just before the spectrometer which was set to only allow the light with the polarization direction parallel to that of the pump laser to pass through. The measured energy of the 391-nm laser shows clear exponential dependence on the plasma length in Fig. 4, as evidenced by the gain curve with an estimated gain coefficient of ∼5.02 cm^{-1}. This gain coefficient is more than one order of magnitude higher than that of the ASE as reported in Ref. [2], due to the completely different pumping mechanisms behind the amplified seed laser and the ASE laser.

The fact that population inversion could be achieved within an ultrafast time scale for initiating subsequent amplification of the third and fifth harmonics indicates that the ionization of the inner-valence electron has occurred during the strong-field ionization of nitrogen molecules. This is because the ejection (ionization) of an inner-valence electron from the $\sigma_u 2s$ orbital of nitrogen molecules leaves the ion in the excited $B\,^2\Sigma_u^+$ state, whereas the ionization of an outer-valence $\sigma_g 2p$ electron leads to the molecular nitrogen ions lying at the ground $X\,^2\Sigma_g^+$ state [19,20].

As shown in Fig. 5(a), these are two distinct channels of ionization: one ionizing the outer-valence electron, resulting in the ground state of the nitrogen molecular ion, and the other ionizing the inner-valence electron, resulting in an excited ionic state. Figure 5(b) shows the detailed transitions in the second channel. The lower potential curve in this case is empty, initially. Thus, any transition from the upper curve to the lower curve would represent that from an inversion system. This mechanism ensures that the population inversion can occur instantly with the ionization of inner-valence electrons, leading to the gain we observed in this channel. On the other hand, the population of the molecular nitrogen ions in the ground state resulting from the other channel could be reduced by absorption of the harmonic photons. As a matter of fact, the lasing wavelengths shown in Fig. 2(b) are located at the long-wavelength side of the harmonic spectra, indicating that the harmonics play an important role in the population inversion. The ground ionic nitrogen molecules will absorb the harmonics which are resonant with some higher vibrotational levels of the excited $B\,^2\Sigma_u^+$ state. This will efficiently reduce the population of the molecular nitrogen ions in the ground state, leading to the population inversion for the transitions indicated in Fig. 5. Thus, the optical harmonics, which have a broad spectrum, simultaneously play two roles for promoting the remote lasing. The first role is the seeding effect, i.e., the spectral portion of the harmonic emission that matches the resonant transition wavelength

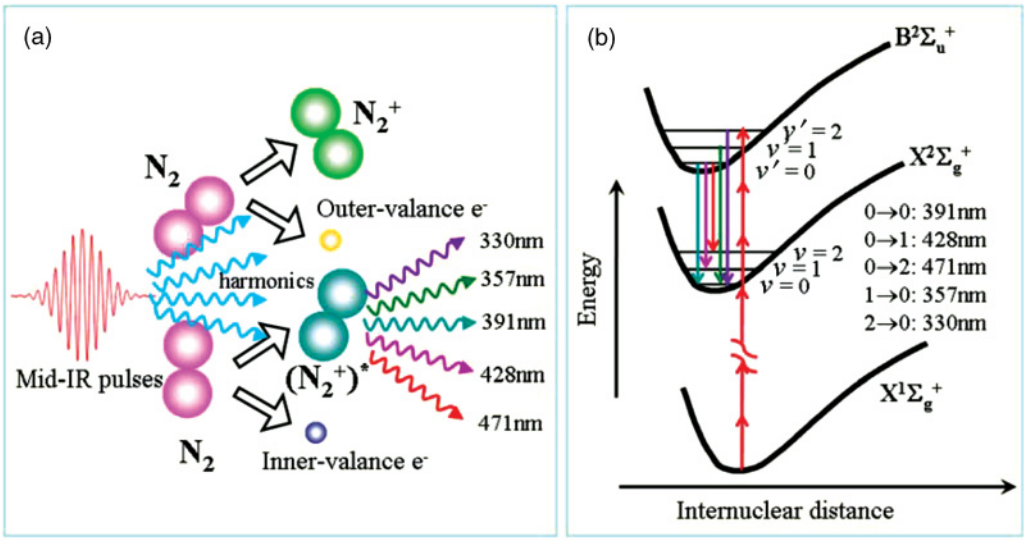

FIG. 5. (Color online) (a) Interaction of nitrogen molecules simultaneously with mid-IR laser field and its third or fifth harmonics resulting in the formation of molecular nitrogen ions at an excited state by ionization of inner-valance electrons, giving rise to a harmonic-seeded laser. (b) Energy-level diagram of ionized and neutral nitrogen molecules in which the transitions between $B\,^2\Sigma_u^+$ and $X\,^2\Sigma_g^+$ states are indicated with corresponding lasing wavelengths.

of N_2 will be amplified. The second role is to reduce the ground-state population, contributed by the spectral portion that has a shorter wavelength than the resonant transition wavelength.

This ultrafast population inversion is unambiguously confirmed from the observed remote lasing seeded by the spectral portions of the third and fifth harmonics that overlap with the gain in inverted nitrogen ions. Interestingly, with this harmonic-seeding mechanism, it would be impossible to achieve the seeded lasing action at 337 nm (i.e., corresponding to $C\,^2\Pi_u$-$B\,^3\Pi_g$ transition of neutral nitrogen molecules) even though there is population inversion [1,2]. This is because the $C\,^3\Pi_u$ state of nitrogen molecules results from the dissociative recombination in a picosecond time scale through the following processes: $N_2^+ + N_2 \Rightarrow N_4^+$; $N_4^+ + e \Rightarrow N_2(C\,^3\Pi_u) + N_2$ [21]. This prediction is confirmed by the fact that no lasing at 337 nm could be observed in our experiment.

In conclusion, we have demonstrated a remote seeded laser (not ASE) in air that can dynamically switch between different wavelengths. Unlike ASE, which depends on the fluorescence lifetime of N_2^+, this seeded laser propagates with the filamenting pump. Hence, lasing action (amplification of the seed) would occur as long as the filament occurs. Future development in the mid-IR ultrafast laser technology will lead to pump pulse with significantly higher energies, by which remote lasers in air with greatly enhanced peak powers and at designated remote locations can be expected. This would provide a toolkit for remote nonlinear spectroscopy applications.

The work is supported by National Basic Research Program of China (Grant No. 2011CB808102), National Natural Science Foundation of China (Grants No. 10974213, No. 60825406, and No. 11074098), and NCET-09-0429. S.L.C. is supported by the Canada Research Chair.

[1] Q. Luo, A. Hosseini, W. Liu, and S. L. Chin, Opt. Photon. News **15**, 44 (2004).
[2] Q. Luo, W. Liu, and S. L. Chin, Appl. Phys. B **76**, 337 (2003).
[3] A. Dogariu, J. B. Michael, M. O. Scully, and R. B. Miles, Science **331**, 442 (2011).
[4] V. Kocharovsky *et al.*, Proc. Natl. Acad. Sci. USA **102**, 7806 (2005).
[5] P. R. Hemmer *et al.*, Proc. Natl. Acad. Sci. USA **108**, 3130 (2011).
[6] H. L. Xu, J. F. Daigle, Q. Luo, and S. L. Chin, Appl. Phys. B **82**, 655 (2006).
[7] S. L. Chin *et al.*, Can. J. Phys. **83**, 863 (2005).
[8] S. L. Chin, F. Théberge, and W. Liu, Appl. Phys. B **86**, 477 (2007).
[9] L. Bergé, S. Skupin, R. Nuter, J. Kasparian, and J.-P. Wolf, Rep. Prog. Phys. **70**, 1633 (2007).
[10] J. Kasparian, R. Sauerbrey, and S. L. Chin, Appl. Phys. B **71**, 877 (2000).
[11] A. Becker *et al.*, Appl. Phys. B **73**, 287 (2001).
[12] W. Liu *et al.*, Opt. Commun. **202**, 189 (2002).
[13] N. Aközbek *et al.*, Phys. Rev. Lett. **89**, 143901 (2002).
[14] F. Théberge, N. Aközbek, W. Liu, A. Becker, and S. L. Chin, Phys. Rev. Lett. **97**, 023904 (2006).
[15] H. Xu *et al.*, Appl. Phys. Lett. **93**, 241104 (2008).
[16] P. Colosimo *et al.*, Nat. Phys. **4**, 386 (2008).

[17] H. Xiong *et al*., Opt. Lett. **34**, 1747 (2009).
[18] Y. Fu *et al*., Opt. Lett. **34**, 3752 (2009).
[19] G. N. Gibson, R. R. Freeman, and T. J. McIlrath, Phys. Rev. Lett. **67**, 1230 (1991).
[20] A. Becker, A. D. Bandrauk, and S. L. Chin, Chem. Phys. Lett. **343**, 345 (2001).
[21] H. L. Xu, A. Azarm, J. Bernhardt, Y. Kamali, and S. L. Chin, Chem. Phys. **360**, 171 (2009).